CFD Modeling of Thermally and Chemically Nonequilibrium Air Flows in Discharge Channel and in Under-Expanded Plasmatron Jets Over a Butt-End Probe

V. I. Sakharov, V. G. Gromov*, A. F. Kolesnikov** and A.N. Gordeev***

**Institute of Mechanics Moscow State University, 1 Michurinskii Pr., 119192, Moscow, Russia*

** Institute for Problems in Mechanics of Russian Academy of Sciences, Prospect Vernadskogo 101/1, 119526, Moscow, Russia

Abstract

The chemically and chemically non-equilibrium flows in a discharge channel of an inductive plasmatron and in under-expanded air jets over a flat-end model are studied by CFD modeling. CFD modeling of entire flow field and heat transfer is carried out for supersonic high-enthalpy air test conditions of the 100-kW inductive plasmatron IPG-4 in the Institute for Problems in Mechanics of Russian Academy of Science (IPM RAS). The results of the code-to-experiment validation in terms of the stagnation point heat transfer rates and stagnation pressure and the flow pattern near the model are reported. The discrepancies in numerical results for various gas-phase models are analyzed.

1. Introduction

The designing of modern space systems poses a set of new issues for science and technology. Aerodynamic heating is the most essential problem and it is strongly influenced by thermochemical nonequilibrium processes and surface catalytic effects. Surface catalysis can contribute essentially in heat transfer rate to vehicle surface during a hypersonic entry to the Earth or Martian atmospheres. Therefore the coupled experimental and numerical study of the surface catalysis in terms of atomic recombination still remains in the list of the most important issues of aerothermophysics.

Inductive plasmatrons are suitable for the study of surface catalysis and simulation of thermochemical interaction of high-enthalpy gas flows with thermal protection materials (TPM) at the hypersonic flight conditions. They are used for the generation of exceptionally pure gas flows with high reproducibility, stability of the free stream conditions and long duration of the plasmatron operation.

CFD modeling as well as experiments is the main tool for the study of the processes and flows in inductive plasmatron discharge channel and in outward jet flows. The joint efforts of CFD modeling and experiments allow extracting of TPM catalysis related to atomic recombination from heat transfer measurements.

The main purpose of the present paper is the demonstration of the CFD codes developed capabilities for the modeling of the entire flow fields and the heat transfer for the supersonic high enthalpy air test conditions of the 100-kW inductive plasmatron IPG-4[1].

1.2 Facility and aerothermal tests

Aerothermal tests in supersonic partially dissociated and ionized airflows were performed of the 100-kW

plasmatron IPG-4 in IPM RAS[1]. The IPG-4 has discharge channel with diameter D_c = 80 mm and the length L_c= 400 mm. The conical sonic nozzles with exit diameters are located at the channel upper interface.

The main IPG-4 parameters in the tests were the following: the generator frequency - f = 1.76 MHz; the powers input in plasma - N_{pl} = 29, 41 kW; the air mass flow rates - G = 2.4, 4.8 g/s; the angle of the input flow swirl was 45^0; the values of ground pressure in the test chamber were sustained at constant level - P_∞ = 6.3, 8.3, 10.3, 12.0 hPa, the sonic nozzle exit diameters were D_s = 30, 40 mm.

The water-cooled copper model of 20 mm in diameter with flat face was used in experimental study of the heat transfer to cooled metallic surfaces. The stagnation point heat fluxes were measured by the steady-state water flow probe made of copper. The measurement accuracy of the stagnation point heat flux to a cooled surface (T_w = 300 K) was of the order of 5% [2].

1.3 Gas-phase, kinetic and transport models

The air is considered as an ideal mixture of perfect gases with corresponding state equation. The gas mixture consists of 11 species: O, N, O_2, N_2, NO, O^+, N^+, O_2^+, N_2^+, NO^+, e^-.

Rotational and vibrational energy modes of molecules are described by the "rigid rotator – harmonic oscillator" model with the Boltzmann distribution of the energy levels. It is supposed that all species are in the ground electronic state and rotational temperature of molecules is equal to translational temperature T.

Two thermally non-equilibrium models have been used in CFD modeling:

- one-temperature model where vibrational and electron temperatures are assumed to be equal to translational temperature T.
- three-temperature model with common vibrational temperatures T_v for molecules O_2, N_2 differed from translational temperature T and electron temperature T_e calculated from the electron gas energy balance equation. The VT, eT and eV energy exchanges were taken into account in the numerical modeling.

1.4 Chemical kinetics

The database of chemical kinetics developed in the Institute of Mechanics MSU was used. In this model the forward rate constant of the reaction of dissociation is presented by the following expression

$$k_j^f = a_j T^{nj}(1 - exp(-\theta_j/T))exp(-E_j/T)$$

Here θ_j is the characteristic vibrational temperature of the j-th molecule. The forward rate constants k_j^f of exchange reactions are approximated by the Arrhenius formula. The reverse rate constants k_j^r are defined from detailed equilibrium condition $k_j^f/k_j^r = K_{n,j}(T)$, where $K_{n,j}(T)$ is the equilibrium constant of the j-th reaction. The numerical parameters of these chemical reactions are listed in [3-6].

1.5 Transport properties

Transport properties are required to describe viscous fluxes of mass, momentum, and energy in gas. The molar diffusion fluxes are determined from the two-temperature Stefan-Maxwell relations for the partially ionized gas mixture including the baro-diffusion terms and the electric field [7]. The diffusion type transport cross sections of atoms and molecules are calculated using two-parametric formulas obtained by the curve fittings on the basis of the cross sections values at low (T=300 K) and high temperature (T=20000 K) [8]. The transport cross sections are evaluated from the Lennard-Jones potential at low temperature and from the exponential repulsive potential at high temperature for pairs of neutral –neutral. The collision integrals are calculated from polarization potential for low temperatures and also from exponential repulsive potential for high temperatures for the pairs of neutral-ion. At the

evaluation of collision integrals of diffusion type for pairs of neutral-parent ion, effect of resonant charge transfer is taken into account.
The interactions of charged particles are described on the basis of the screened Coulomb potential. The collision integrals for pairs of electron-atom are 1.5 Å^2 and for pairs of electron-molecule are 4.0 Å^2.
The values of potential parameters for the identical particles are taken from the published data. Parameters of potentials for other particles are determined by combinatorial rules. It is supposed that the ratios of all viscosity and diffusion types of cross sections are equal to 1.1. The viscosity and thermal conductivity of air mixture are calculated by approximate Wilke-Vasiliyeva type formulas [9].

2. CFD modeling nonequilibrium air flow

2.1 Numerical method

This problem has been solved on the basis effective numerical technique for high temperature gas flows simulation (HIGHTEMP) developed in Institute of Mechanics MSU [10].
The quasi 3-D system of the time-dependent full Navier-Stockes (N-S) equations [11] are integrated on the multi-block structured mesh using a finite volume approach. Under this approach, the finite difference equations system consists of numerical analogs of the governing equations for quadrilateral cells covering the computation domain and difference approximation of the boundary conditions.
The inviscid fluxes across cell faces are calculated basing the result of the exact Riemann problem solution. The numerical viscous fluxes through cell sides are evaluated using the central and one-sided difference formulas of the second order of accuracy. The steady-state solution is defined due to the implicit iterative procedure. The flowfield parameters are computed due to Gauss-Seidel line relaxation numerical method on the every iteration.

2.2 Inductively coupled plasma modeling

This problem has been solved on the basis N-S equations coupled with the simplified Maxwell equation for the RF electromagnetic field. Simplified quasi 1D Maxwell equations for the complex amplitude of the tangential component of the electric field generating vortical electric currents were solved for the discharge channel [12].
The input parameters of the problem are the inductor current frequency f, the gas flow rate G, the power input in plasma N_{pl}, the ground pressure P_∞ and gas temperature T_∞ in the test chamber and exit diameter D_s of the sonic nozzle. The mentioned input parameters correspond to the aerothermal IPG-4 test conditions.
The flow streamlines and translational temperature fields for the air plasma in the plasmatron discharge channel are shown in Fig. 1. The calculations are presented for one-temperature gas-phase model. The complicated structure of the flow with embedded vortical zones is formed in the center of the discharge channel. The cold gas goes along the discharge channel wall. The form of the separation zones depends on diameter of sonic nozzle exit.

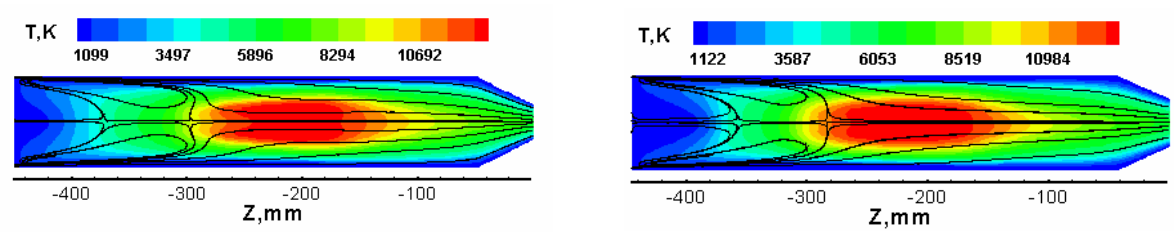

a) b)

Figure 1: The flow streamlines and translational temperature contours in the plasmotron discharge channel
P_∞ = 12 hPa T_∞= 293 K G = 4.8 g/s N_{pl} = 41 kW a) D_s = 30 mm b) D_s = 40 mm

Fig.2 demonstrates also the vibrational and electron temperature contours in the discharge channel obtained in the framework of the three-temperature gas-phase model. The vibrational temperature T_v maximum is about 30000K in the heating area. The difference between T_v and T_e maximums is of the order of 2800K. The calculated translational temperatures were close to each other in the considered gas-phase models. The vibrational and electron temperatures obtained in the framework of three-temperature model used are essentially differed from the translational ones.

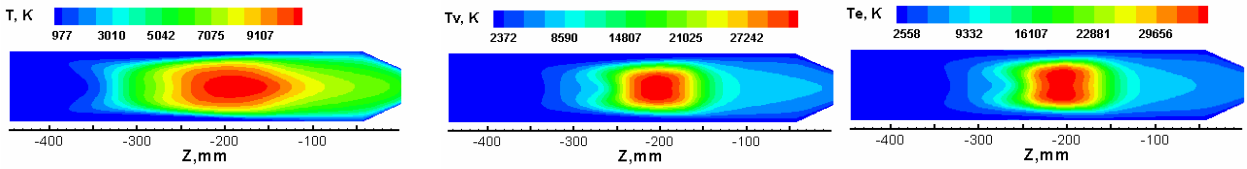

a) b) c)

Figure 2: The translational (a), vibrational (b) and electron(c) temperature contours in the plasmotron discharge channel

P_∞ = 6.3 hPa T_∞= 293 K G = 2.4 g/s N_{pl} = 29 kW D_s = 40 mm

Fig.3 also demonstrates the translational, the vibrational and the electron temperature contours in the discharge channel for other set parameters in the experiment. It is observed more pressure value in the discharge channel in comparison with test regime presented in the Figure 2. The translational *(T)*, vibrational *(T_v)* and electron *(T_e)* temperature values in the heating area are closer to each other in this case. The difference between T_v and T_e maximums is of the order of 400K. The vibrational and electron temperatures obtained are not essentially differed from the translational one.

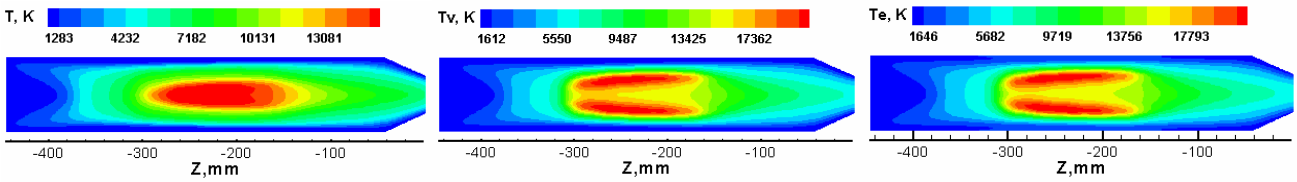

a) b) c)

Figure 3: The translational (a), vibrational (b) and electron(c) temperature contours in the plasmotron discharge channel

P_∞ = 12 hPa T_∞= 293 K G = 4.8 g/s N_{pl} = 41 kW D_s = 40 mm

2.3 Calculation results of the flow over the butt-end model

The CFD results were found to be in a good agreement with the experimental geometry of the under-expanded free air jets. We note that the flow pattern over model strongly depend both the ground pressure P_∞ in the test chamber and the model location Z_m in the jet.

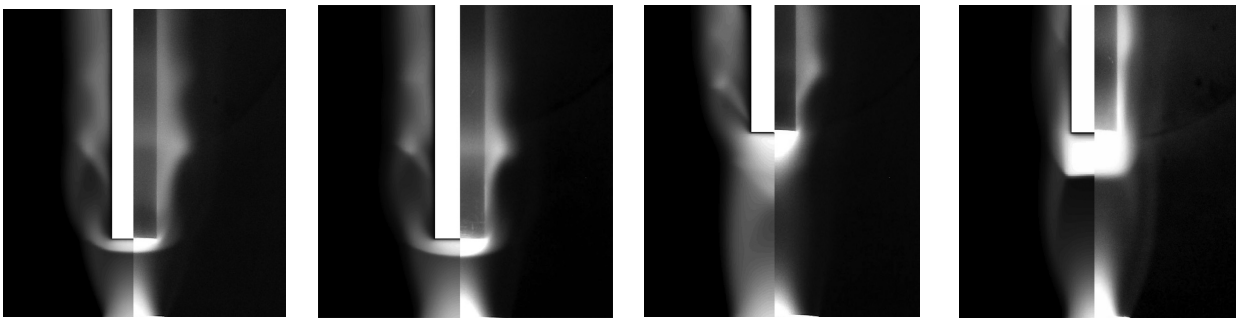

a) b) c) d)

Figure 4: The under-expanded supersonic plasma air jet flow over flat-end cylindrical model
The right part is the experiment; the left one is the shadow of computational picture

a) P_∞ = 8.3 hPa G = 2.4 g/s N_{pl} = 41 kW D_s = 30 mm Z_m = 30 mm
b) P_∞ = 8.3 hPa G = 2.4 g/s N_{pl} = 29 kW D_s = 40 mm Z_m = 20 mm
c) P_∞ = 10.3 hPa G = 2.4 g/s N_{pl} = 29 kW D_s = 40 mm Z_m = 70 mm
d) P_∞ = 12 hPa G = 4.8 g/s N_{pl} = 41 kW D_s = 30 mm Z_m = 70 mm

For the regime, presented in Fig. 4c) the flow does not separate in front of the model for all model locations in the jet; a straight shock wave is observed as a result of non-uniform supersonic flow in front of the model.
For the regime presented in Fig. 4 d), the subsonic separation zone is formed in front of the flat-end probe located of 70 mm from the nozzle exit. It changes heat transfer with the model.
Fig.5 demonstrates the Mach contours over the butt-end probe located at 100 mm from the nozzle exit. The model is located sufficiently far from the nozzle exit and it does not affect on the jet flow in the initial section near the nozzle. In the regime corresponded to Fig. 5b), the flow does not separate in front of the model for all model locations in the jet. The subsonic separation zones are observed in front of the model for test regime presented in Fig. 5 a) and this could affect on the heat transfer to the model.

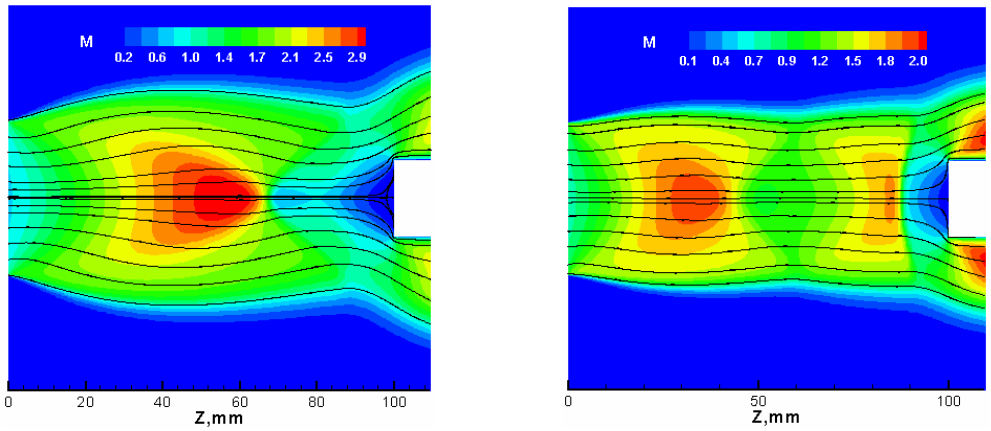

Figure 5: Mach contours and the flow streamlines in supersonic airflow over butt-end model

a) P_∞ = 6.3 hPa T_∞= 293 K G = 2.4 g/s N_{pl} = 29 kW D_s = 40 mm
b) P_∞ = 10.3 hPa T_∞= 293 K G = 2.4 g/s N_{pl} = 29 kW D_s= 40 mm

The Fig.6 demonstrates the Mach contours over the butt-end probe located at 80 mm from the nozzle exit for thermally equilibrium and non-equilibrium gas-phase model correspondently.

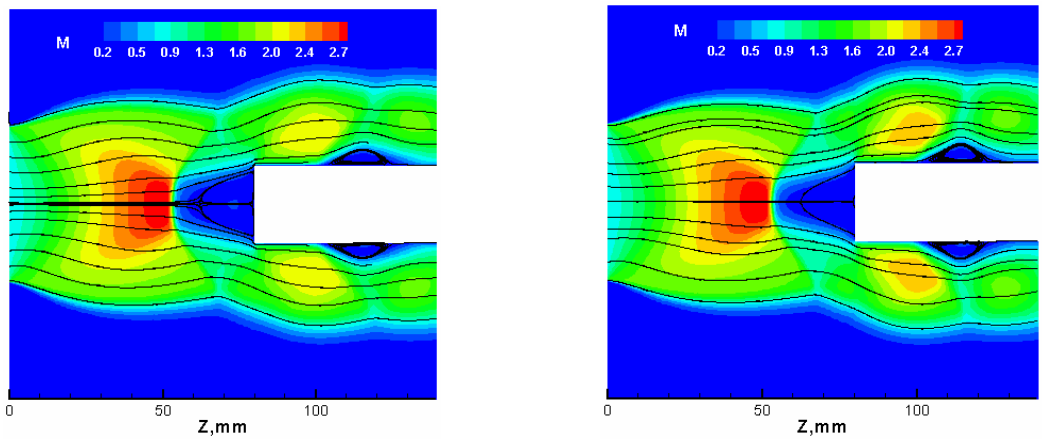

Figure 6: Mach contours and the flow streamlines in supersonic airflow over butt-end model
P_∞ = 12 hPa T_∞= 293 K G = 4.8 g/s N_{pl} = 41 kW D_s = 40 mm
a) thermally equilibrium model b) thermally non-equilibrium model

We note that the flow topology slightly depends on the gas-phase model used. The separation zone is less and the supersonic jet is narrower for the thermally non-equilibrium model.

Non-monotonous stagnation point heat fluxes and stagnation pressure distributions along the jet axis discovered experimentally were confirmed by the CFD modeling (Fig.7-8). The calculated local minima and maxima in the heat flux and pressure distributions coincide well with the experimental data. Local maxima and minima correspond to supersonic flow and subsonic separated-flow over the model correspondingly. The heat fluxes were calculated for the catalytic efficiencies $\gamma_O=\gamma_N$ = 0.1 corresponding to the recombination of oxygen and nitrogen atoms on the copper surface [13].

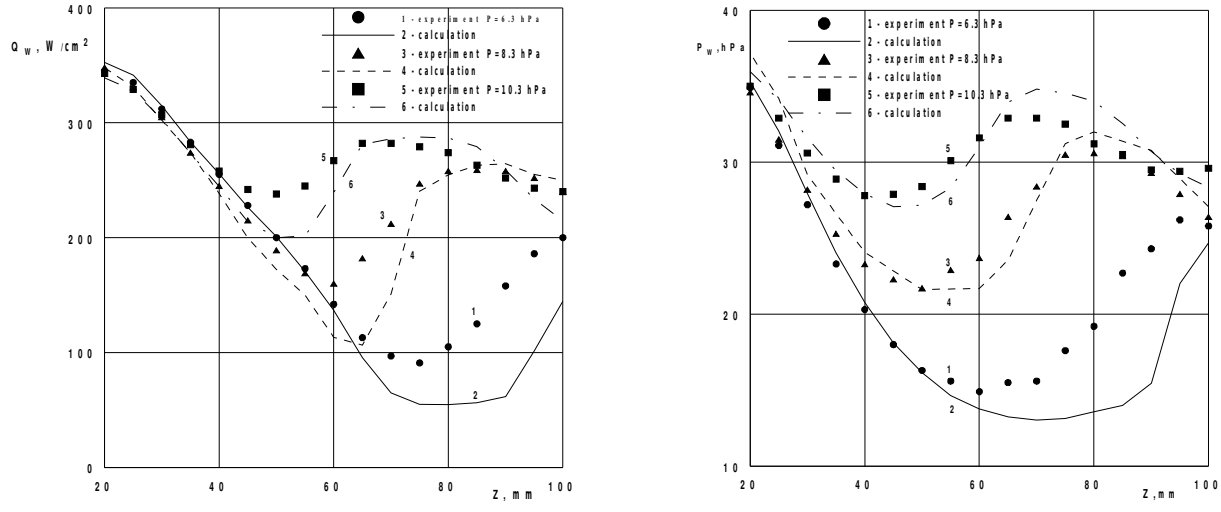

Figure 7: The comparison of the calculated and experimentally measured heat fluxes and stagnation pressure distributions along the jet axis for the cupreous surface for the follow IPG-4 test parameters:
G = 2.4 g/s N_{pl} = 29 kW D_s = 40 mm 1,2 - P_∞ = 6.3 hPa 3,4 - P_∞ = 8.3 hPa 5,6 - P_∞ =10.3 hPa
1, 3, 5 – experiment 2, 4, 6 – calculations

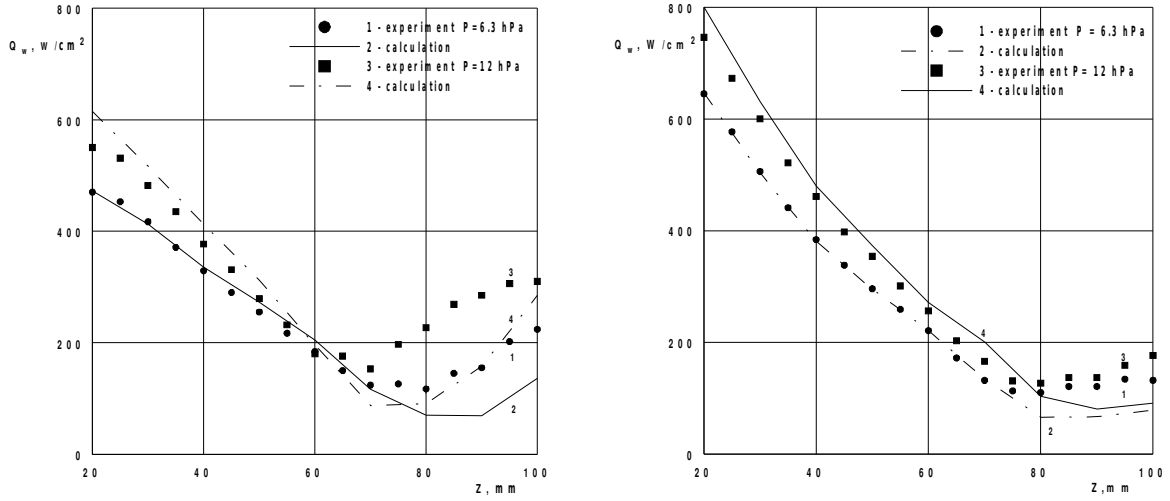

Figure 8: The comparison of the calculated and experimentally measured heat fluxes distributions along the jet axis for the cupreous surface for the follow IPG-4 test parameters: N_{pl} = 41 kW
1,2 - P_∞ = 6.3 hPa, G = 2.4 g/s 3,4 - P_∞ = 12 hPa, G = 4.8 g/s a) D_s = 40 mm b) D_s = 30 mm
1, 3 – experiment 2, 4 – calculations

We note that the copper surface did not appear itself as the fully catalytic one for supersonic jet flow unlike the case of subsonic high enthalpy airflows [14].
The difference between heat fluxes obtained in the frameworks of various gas-phase models is observed for the butt-end probe location of the order of 60 mm from the nozzle exit (curves 2 and 3). In this case the subsonic flow over the body is realized and the pressure in front of the butt-end probe is smaller than in the case of supersonic flows. Therefore the energy exchange between of translational and vibrational degrees of freedom decelerates. As a result the higher translational gas temperature near the body surface causes the higher heat flux values.

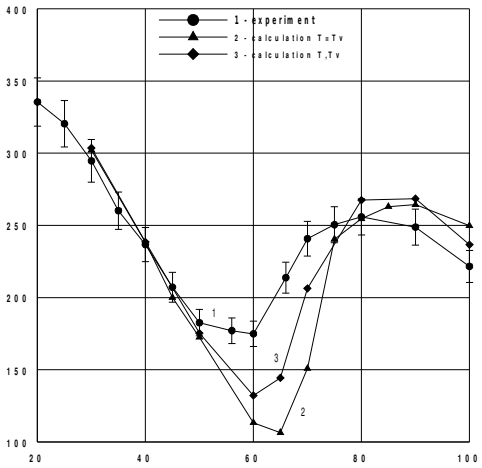

Figure 9. The comparison of the calculated heat fluxes distributions along the jet axis for one- and multi-temperature gas-phase models: G = 2.4 g/s, N_{pl} = 29 kW, P_∞ = 8.3 hPa, D_s = 40 mm
1 – experiment ; 2 (one-temperature model), 3 (three-temperature model) - calculations

Conclusion

Under-expanded air free jets and heat transfer in supersonic flows under the IPG-4 plasmatron (IPM) test conditions are studied by CFD modeling.

The difference between the calculated electron-vibrational and translational temperatures in plasmotron discharge channel for considered test conditions is in agreement with the physics of energy transfer from electric field to the airflow.

The CFD results were found to be in a good agreement with the experimental geometry of the under-expanded free air jets.

Non-monotonous stagnation point heat flux and pressure distributions along the jet axis observed in the experiment are confirmed by CFD modeling. The calculated distributions of the stagnation point heat fluxes, stagnation pressure and locations of the local minima and maxima are found to be in agreement with the experimental data.

Calculated stagnation point heat fluxes and pressure weakly depend on the used gas-phase models for supersonic flow over the butt-end probe. The heat fluxes calculated using one-temperature and multi-temperature gas-phase models are in worse agreement for subsonic flow over the butt-end probe.

The copper cannot be considered as a fully catalytic material in supersonic jet flows, particularly, for the flow enthalpy rebuilding on the basis of the measured stagnation point heat flux.

This work was supported by the RFBR grant (project project 05-01-00844)), by the INTAS (INTAS-CNES project 03-53-5117), by the basic research program of Presidium RAS (project 09), and performed under contract to the International Science and Technology Center (ISTC), Moscow.

References

[1] Yakushin M. at al. A. Mass Loss of SiC Sample Surfaces under Different Flow Conditions // AIAA 98-2605. June 1998.

[2] Gordeev A.N., Kolesnikov A.F., Kononov S.V. Comparative characterization of the IPG-4 inductive plasmatron in subsonic and supersonic regimes of air plasma flows // Proc. Int. Conf. on Methods of Aerophysical Research (ICMAR 2004). Novosibirsk , Russia. 2004. Publishing House "Nonparel". Part I. P. 106-111.

[3] Ibragimova L.B., Smekhov G.D., Shatalov O.P. Dissociation rate constants of diatomic molecules under thermal equilibrium conditions // Fluid Dynamics. 1999. V. 34. No 1. P.153-157.

[4] Losev S.A.., Makarov V.N., Pogosbekyan M.Yu. Model of the physico-chemical kinetics behind the front of a very intense shock wave in air // Fluid Dynamics. 1995. V. 30. No 2. P.299-309.

[5] Park C. Review of chemical-kinetic problems of future NASA missions, Earth Entries // J. Thermophys. and Heat Transfer. 1993. V.7. No.3. P.385-398.

[6] Losev, S.A., Makarov V.N., Pogosbekyan M.Ju., Shatalov O.P., Nikol'sky V.S. Thermochemical nonequilibrium kinetic models in strong shock waves on air // 1990. AIAA. Paper. 1994. No 1990.

[7] Kolesnikov A.F. Steffan-Maxwell Relations for Multicomponent Ambipolar Diffusion and Thermal-Baro-Diffusion Effects in Two-Temperature Plasmas // 2000. AIAA 2000-2570.

[8] Afonina N.E.,Gromov V.G. Thermochemical Nonequilibrium Computations for a MARS express Probe // Proc. 3-rd Europ. Sympo. on Aerothermodynamics for Space Vehicles, ESTEC, Noordwijk. The Netherlands. 1998. P. 179-186.

[9] Reid R.C., Prausnitz J.M.,Sherwood T.K *The Properties of Gases and Liquids,* McGraw-Hill, N.Y.:1977.688 p.

[10] Afonina N.E., Gromov V.G., Sakharov V. I. HIGHTEMP technique for high temperature gas flows simulations // Proc. 5th Europ. Sympo. on Aerothermodynamics for Spase Vehicles. Cologne, Germany. 2005. SP 563. P. 323-328.

[11] Sakharov V. I. et al. CFD Model and Code-to-Experiment Validation for An Under-Expanded Nonequilibrium Plasmatron Jet Over A Butt-End Probe // West East High Speed Flow Field 2002. CIMNE Barcelona, Spain. 2003. P. 144-150.

[12] Vasil'evskii S.A. and Kolesnikov A.F, Numerical simulation of equilibrium induction plasma flows in a cylyndrical plasmatron channel // *Fluid Dynamics.* 2000. Vol. 35. P.769.

[13] M.Barbato, S.Reggian, C.Bruno and J.Muylaert Model for Heterogeneous Catalysis on Metal Surfaces with Applications to Hypersonic Flows // Journal of Thermophysics and Heat Transfer. 2000. Vol.14. No. 3. P.412-420.

[14] Kolesnikov A.F. The Aerothermodynamic Simulation in Sub- and Supersonic High-Enthalpy Jets: Experiment and Theory //Proc. of the 2nd European Symp., on Aerothermodyn.. for Space Vehicles // ESA SP-367. 1995. P. 583 -588.

This page has been purposedly left blank